PHYSICAL REVIEW D VOLUME 22, NUMBER 7 1 OCTOBER 1980

Quark jets in pion diffractive dissociation

J. Randa
Department of Physics, University of Colorado, Boulder, Colorado 80309
(Received 23 May 1980)

The cross section for diffractive dissociation of the pion into a high-mass system clearly separated in momentum space from other final-state particles is calculated using two-gluon exchange between the pion's quark-antiquark and the target. Two-jet behavior for the pion-fragment subsystem is predicted and the dependence on jet angle and on the mass of the diffractively excited system is calculated. Comparisons are made to an earlier calculation of the analogous photon-induced process, and the magnitudes of both cross sections are estimated and found to be sufficiently large to measure.

I. INTRODUCTION

The diffractive photoproduction of quark-antiquark ($q\bar{q}$) pairs has recently been treated in the context of perturbative quantum chromodynamics (QCD).[1] The mechanism studied in Ref. 1 (hereinafter referred to as KDR) is one in which the incident photon couples in a pointlike manner to a $q\bar{q}$ pair which then scatter from the target proton via two-gluon exchange. The principal reason for exchanging two gluons rather than one, which had been studied previously,[2] was to facilitate identification of the $q\bar{q}$ system, thereby focusing on fragments of the photon alone. The final-state configuration considered was one in which the recoil proton (in $\gamma p \to Xp$) had the smallest longitudinal momentum in the laboratory frame and was separated by a large rapidity gap from any other final-state particle, e.g., the proton alone in one center-of-mass (c.m.) hemisphere and N pions in the other. Such a configuration allows the pions to be identified as fragments of the beam (photon), and the pion system can then be subjected to exactly the same jet analyses as in e^+e^- annihilation into hadrons. It was argued by KDR that such events arise from the exchange of a color singlet ($q\bar{q}$ or gg) rather than from one-gluon exchange. The latter produces two color-octet systems, and the subsequent *soft* color neutralization and hadron formation should not lead to large holes in momentum space. (A more detailed argument in the context of e^+e^- annihilation can be found in Ref. 3.)

The photon-induced reaction is a particularly convenient case to study because the coupling of a photon to $q\bar{q}$ is known, provided we are considering a short-distance (sub)process. If both $t \equiv (p_\gamma - p_X)^2$ and $M^2 \equiv p_X^2$ are large, then a hard subprocess is assured; in addition, KDR made a case for large M^2 being sufficient, even for small $|t|$. They then calculated cross-sections differential in M^2 and in $\cos\theta^*$, where θ^* is the angle between the quark jet and the incident photon in the $\vec{p}_X = 0$ frame. In order to do so it was necessary to assume a particular form for the elastic two-gluon form factor of the proton. It was expected, however, that the details of the fragments of the photon would be relatively insensitive to the nature of the target, and this did indeed prove to be the case in KDR's calculation.

This paper will treat the analogous pion-induced reaction. There are two obvious qualitative differences in the two calculations: The pion coupling to $q\bar{q}$ is not pointlike, and furthermore it is not known. The lack of a hard component in the $\pi q\bar{q}$ coupling we would expect to see reflected in some feature (e.g., M^2 dependence) of the pion cross-section results when compared to the photoproduction predictions. The second difference is no longer an insuperable problem since the behavior of the pion form factor when one quark is highly virtual has now been calculated.[4] Since we did not know the $\gamma q\bar{q}$ coupling when neither quark was highly virtual, we are in qualitatively similar situations in photon and pion fragmentation.

We are therefore in a position to calculate $\pi p \to Xp$, where the proton is the slowest final-state particle (in the laboratory) and is well separated in rapidity from any particle in X. In fact, since the results depend only weakly on the proton side, there would be little difference if we replaced the $ggpp$ vertex by a $ggpX'$ vertex (although we might want to change the t dependence of the proton form factor). We can then calculate $\pi p \to XX'$, where the X and X' systems are separated by a sizeable rapidity gap, and similarly we can obtain predictions for the analogous photoproduction process $\gamma p \to XX'$. In addition, we will estimate the overall normalization for both pion- and photon-induced processes in order to get some idea of the values of M^2 for which it is feasible to measure these cross sections.

The outline of the remainder of the paper is as follows. In the next section, we review briefly the

salient features of the photoproduction calculation of KDR, establishing our notation in the process. Section III contains the body of the calculation and presents the results, which are discussed in Sec. IV. There is also one appendix, containing details of the normalization estimates.

II. NOTATION AND PHOTOPRODUCTION REVIEW

The diagrams calculated in Ref. 1 are shown in Fig. 1(a), where the blobs on the right-hand side were originally the subgraphs of Fig. 1(b). When the blob is given by Fig. 1(b), then the graphs of Fig. 1(a) are the leading order in α_s of those which are leading order in $\sqrt{s}$. Using Fig. 1, one is actually calculating photon fragmentation from a meson target, but if the fragmentation is approximately target independent this will not matter. (We will see below that this is the case.) The calculation is done in the limit $s \gg M^2$, $|t|$, m_i^2, where $s=(p_1+p_2)^2$, $M^2=(q_1+q_2)^2$, $t=(p_1-p_3)^3 \equiv K^2$. In order to have the $q\bar{q}$ form visible jets, and as a necessary condition for the application of perturbation theory, we also require $M^2 \gg m_i^2$, but we do not use this fact to neglect nonleading terms in m_i^2/M^2.

Infinite-momentum techniques (see, e.g., Ref. 5) are employed in the evaluation of the amplitude. For this purpose it is convenient to use light-cone coordinates,

$$\begin{aligned} &a^\mu=(a^+,a^-,\vec{a}_\perp)\ , \\ &a^\pm=(1/\sqrt{2})(a^0\pm a^3)=a_\mp\ , \\ &a\cdot b=a_+b_-+a_-b_+-\vec{a}_\perp\cdot\vec{b}_\perp\ . \end{aligned} \tag{1}$$

Following Ref. 5, the external momenta are written as

$$\begin{aligned} &p_1^\mu=P^\mu-K^\mu/2,\quad p_3^\mu=P^\mu+K^\mu/2\ , \\ &p_2^\mu=Q^\mu+K^\mu/2,\quad p_4^\mu=q_1^\mu+q_2^\mu=Q^\mu-K^\mu/2\ . \end{aligned} \tag{2}$$

Axes can then be chosen so that (in the overall c.m.)

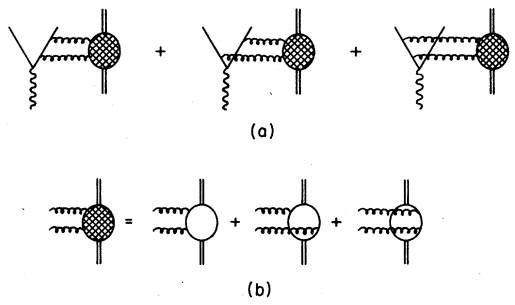

FIG. 1. (a) Dominant graphs for $\gamma p \to 2$ jets $+ p$ in the kinematic region considered. (b) Model used for $ggpp$ vertex.

$$\begin{aligned} &K_+=-(M^2-m_2^2)/\sqrt{2s}\ ,\quad P_+=Q_-=\sqrt{s/2}\ , \\ &K_-=O(s^{-3/2}),\quad P_-=(m_1^2-t/4)/\sqrt{2s}\ , \\ &K_x=K_\perp=\sqrt{-t},\quad Q_+=(M^2-t/4)/\sqrt{2s}\ , \end{aligned} \tag{3}$$

to leading order in $s^{1/2}$, where $p_i^2=m_i^2$. Written in this form, Eq. (3) applies to either photon or pion fragmentation. It is also convenient to introduce the x variables for the q and $\bar{q}$,

$$\begin{aligned} &x_1\equiv q_{1-}/p_{2-}\simeq 2q_1\cdot p_1/s\ , \\ &x_2\equiv q_{2-}/p_{2-}\simeq 2q_2\cdot p_1/s\ . \end{aligned} \tag{4}$$

The invariant amplitude calculated from Fig. 1 takes the form

$$\begin{aligned} &\mathfrak{M}=\sum_{i=1}^{3}\mathfrak{M}_i\ , \\ &\mathfrak{M}_i=C_\gamma\int\frac{d^4k_1d^4k_2}{(2\pi)^4}\,\delta^4(K-k_1-k_2)\,\frac{1}{k_1^2+i\varepsilon} \\ &\qquad\times\frac{1}{k_2^2+i\varepsilon}\,L^i_{\nu\lambda}\,\mathfrak{R}^{\nu\lambda}\ , \end{aligned} \tag{5}$$

where $L^i_{\nu\lambda}$ and $\mathfrak{R}^{\nu\lambda}$ come, respectively, from the left and the right sides of the graphs, and C_γ comprises the coupling constants, color factors, etc.,

$$C_\gamma=\frac{2i}{3\sqrt{3}}\,e_q g_s^{\,4} g_\phi^{\,2}\ , \tag{6}$$

with g_ϕ the target meson $q\bar{q}$ coupling constant and g_s the running coupling constant, evaluated at the large mass scale. (The appropriate mass scale is discussed below.)

The right-hand side of the diagrams, $\mathfrak{R}^{\nu\lambda}$, is calculated from Fig. 1(b). The only component of $\mathfrak{R}^{\nu\lambda}$ which is leading order in s is $\mathfrak{R}^{--}$. For a scalar or pseudoscalar target and recoil particle, $\mathfrak{R}^{--}$ is given by

$$\begin{aligned} &\mathfrak{R}^{--}=\left(\frac{s}{2}\right)^{1/2}\frac{1}{2\pi}\,\delta(k'_-)[I_1(\vec{k}')-I_2]\ , \\ &k_1=k'+K/2,\quad k_2=-k'+K/2\ , \end{aligned} \tag{7}$$

where I_1 and I_2 are two complicated integrals whose exact form need not concern us but which do have the following important features:

$$[I_2(k')-I_1]\sim k'-K/2\ ,\quad \text{as } \vec{k}'\to\pm\vec{K}/2\ , \tag{8a}$$

$$[I_2(k')-I_1]\sim\text{const (modulo logarithms)},\quad \text{as } k'\to 0,\infty\ , \tag{8b}$$

$$[I_2(k')-I_1]\to -2+f(k'/K,\ \cos\theta_{k'K}),\quad \text{as } \vec{K}^2\to\infty\ . \tag{8c}$$

Property (8a) means that $\mathfrak{R}^{--}$ vanishes (linearly) as either of the exchanged gluons becomes soft. This occurs because we are considering the scattering of color singlets. The behavior as $\vec{K}^2 \to \infty$ arises because we used an elementary meson $q\bar{q}$ coupling for the target; it is not what we would expect for physical hadrons.

Equation (7) can be inserted into Eq. (5) and the $\mathfrak{M}_i$'s calculated. Since $\mathfrak{R}^{--}$ is the leading component, only L_{i--} need by considered, provided no components of $L_i^{\nu\lambda}$ are higher order in $\sqrt{s}$ than

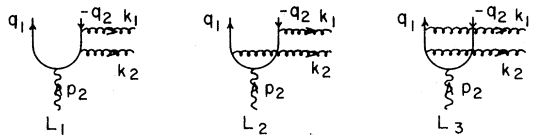

FIG. 2. Details of the fragmentation side of diagrams.

L_{i--}, which is the case. The L_{i--} and, consequently, the $\mathfrak{M}_i$ are obtained from Fig. 2, leading to the result

$$\tfrac{1}{2}\sum_{\text{spins}}|\mathfrak{M}|^2 = -C_\gamma' s^2\Big\{\mathfrak{s}_1^2\Big[\frac{A(1,2)}{(q_1\cdot p_2)^2}+\frac{A(2,1)}{(q_2\cdot p_2)^2}+\frac{A'}{q_1\cdot p_2\, q_2\cdot p_2}\Big]+\mathfrak{s}_2^{\,2}B+8x_1x_2(x_1^{\,2}+x_2^{\,2})\mathfrak{s}_3^{\mu}\mathfrak{s}_{3\mu}$$
$$+\mathfrak{s}_1\mathfrak{s}_2\Big[\frac{D(1,2)}{q_1\cdot p_2}+\frac{D(2,1)}{q_2\cdot p_2}\Big]+\mathfrak{s}_1\mathfrak{s}_3^{\mu}\Big[\frac{E_\mu(1,2)}{q_1\cdot p_2}+\frac{E_\mu(2,1)}{q_2\cdot p_2}\Big]$$
$$+\mathfrak{s}_2\mathfrak{s}_3^{\mu}F_\mu+\mathfrak{s}_1\mathfrak{s}_4\,32x_1x_2\Big(\frac{x_2}{q_1\cdot p_2}+\frac{x_1}{q_2\cdot p_2}\Big)+64x_1^{\,2}x_1^{\,2}\mathfrak{s}_2\mathfrak{s}_4\Big\}\,, \tag{9}$$

where the various coefficients are given by

$$C_\gamma'=\frac{4Q_q^{\,2}}{27\pi}\alpha\alpha^2{}_\phi\alpha^4{}_s,\quad A(i,j)=-16x_j(q_i\cdot p_2+x_j m_q^{\,2})\,,$$
$$A'=16[x_2^{\,2}q_1\cdot K+x_1^{\,2}q_2\cdot K+x_1x_2(p_2\cdot K-2m_q^{\,2})]\,,$$
$$B=8x_1x_2[-8x_1x_2(M^2/2+t/4+m_q^{\,2})+4(x_1-x_2)(x_1q_2\cdot K-x_2q_1\cdot K)-t(x_1^{\,2}+x_2^{\,2})]\,, \tag{10}$$
$$D(i,j)=-16x_j\{x_ix_j[(3q_i+q_j)\cdot p_2+4m_q^{\,2}+t/2]+x_i^2[(2q_i-q_j)\cdot p_2+M^2/2]+x_j^{\,2}(M^2/2-q_i\cdot p_2)\}\,,$$
$$E_\mu(i,j)=-4x_j[d_\mu(i,j)-3x_i^{\,2}+x_j^{\,2})K_\mu],\quad d_\mu(i,j)=\begin{cases}(q_i-q_j)_\mu, & \mu=1,2\\ 0, & \mu=\pm\,,\end{cases}$$
$$F_\mu=-8x_1x_2[d_\mu(1,2)-(x_1-x_2)K_\mu]\,.$$

The integrals $\mathfrak{s}_i$ which occur are

$$\mathfrak{s}_1=\int d^2k'f(k'),\quad \mathfrak{s}_2=2\int d^2k'f(k')\mathfrak{D}^{-1},\quad \mathfrak{s}_{3\mu}=4\int d^2k'f(k')\,k'_\mu\,\mathfrak{D}^{-1},\quad \mathfrak{s}_4=-2\int d^2k'f(k')\vec{k}'^2\,\mathfrak{D}^{-1}\,,$$
$$f(k')=(\vec{k}'+\vec{K}/2)^{-2}(\vec{k}'-\vec{K}/2)^{-2}[I_1(k')-I_2]\,, \tag{11}$$
$$\mathfrak{D}=[M^2x_1x_2+x_1(\vec{k}'+\vec{K}/2)^2+x_2(\vec{k}'-\vec{K}/2)^2+2x_1\vec{q}_2\cdot(\vec{k}'+\vec{K}/2)-2x_2\vec{q}_1\cdot(\vec{k}'-\vec{K}/2)]\,.$$

This result is presented in (nearly) full detail because some of the details are pertinent to the discussion later and because the normalization conventions are somewhat different from those of KDR. The differential cross section is given by

$$\frac{d\sigma}{dM^2d\cos\theta^*}\simeq\frac{1}{2^6(2\pi)^4s(s-M^2)}$$
$$\times\int dt\,d\phi^*\Big(\tfrac{1}{2}\sum|\mathfrak{M}|^2\Big)\,, \tag{12}$$

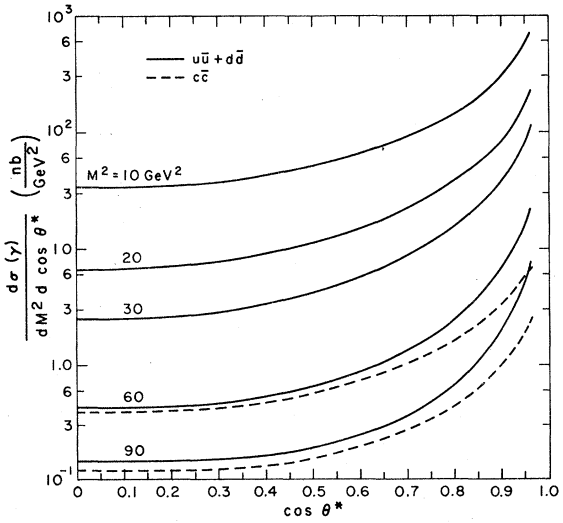

FIG. 3. Predictions for $\gamma p \to q\bar{q}p$ at $s = 300$ GeV^2, including estimated normalization. Cross sections are integrated over all t.

where θ^* is the angle between $\vec{q}_1$ and $\vec{p}_2$ in the $\vec{q}_1 + \vec{q}_2 = 0$ frame and ϕ^* is the angle between $\vec{q}_1$ and the plane defined by $\vec{p}_1$ and $\vec{p}_3$ in the same frame.

The differential cross section was evaluated numerically by KDR (up to an overall normalization), and its properties studied. A number of the general features can be understood from Eqs. (9)–(12) and we shall return to these equations in the discussion following the pion-fragmentation calculation.

Before going on to pion diffractive dissociation, we present in Fig. 3 some representative photoproduction predictions.[6] This will facilitate comparison of the two sets of results, but we also include this figure because it contains normalization estimates (obtained in the Appendix) which were not in KDR. We note that for light $(u+d)$ quark jets the cross sections are quite measurable to very large M^2, whereas for charmed quark jets (which only begin appearing at larger M^2) the cross sections are smaller and will pose something of a challenge to anyone trying to measure them over the full range of θ^*. An interesting point made by KDR is that at $\cos\theta^* \simeq 0$, the cross sections for the different quarks are in proportion to their charges squared, since all mass effects have died out by then. The normalization should not be regarded as a serious prediction, but merely as an indication that the cross sections should be measurable.

III. PION CALCULATION

We now turn to pion fragmentation. A $q\bar{q}$ pair, bound to form a pion, is incident with very high energy upon a proton target. The $q\bar{q}$ scatter into a state of high invariant mass (although $M^2 \ll s$), while the proton recoils elastically. The final-state configuration we have chosen (large separation in momentum space between recoil proton and all other debris) allows identification of all the final-state particles except the proton as fragments of the pion and requires a color singlet to be exchanged between the incident pion and proton. The large invariant mass of the diffractively excited $q\bar{q}$ state ensures that there was a highly virtual intermediate-state quark [see below, Eq. (14)], provided the final-state $q\bar{q}$ are not collinear with the incident pion. This highly virtual quark gives us a short-distance subprocess (π + exchange $\to \pi$ fragments), and we proceed to apply perturbation theory. When $|t|$ is large the justification of perturbation theory can be made quite firm,[1] but our normalization estimates below offer no hope of measuring this process at large $|t|$.

Color-singlet exchange and lowest-order perturbation theory lead us to two-gluon exchange ($q\bar{q}$ exchange is suppressed by $1/s$). The subprocess of interest is then $\pi + 2g \to q + \bar{q}$. The target proton merely serves as a source of the two glouns from which the incident $q\bar{q}$ scatter. We do not know the $ggpp$ vertex; however, as long as we do not try to predict t dependence we do not need to know it. We expect the features of pion fragmentation to be insensitive to what it is that induces the fragmentation, and KDR showed that this was (approximately) the case in photoproduction. In the present calculation we will use their phenomenlogical $ggpp$ vertex.

The first obstacle to calculating pion fragmentation is determination of the coupling between a pion and a quark-antiquark pair. An appealing possibility would be to treat this in the manner used by Berger and Brodsky[7] in calculating quark structure functions in πp Drell-Yan production. They obtain the meson wave function for large momentum transfer from single- (hard-) gluon exchange between the q and $\bar{q}$. When one uses this approach with two-gluon exchange, however, gauge invariance requires an unwieldy number of diagrams; and by the time one reaches the numerical evaluation stage the bookkeeping problem is sufficiently formidable that one person's results could not be trusted. In addition, some of our numerical results will include kinematic regions where the quark and antiquark are not highly virtual, and we would like to have some way of using a more appropriate pion wave function or form factor in those regions. We therefore settle on an effective form for the $\pi q\bar{q}$ vertex given by

$$V(\pi q_1 \bar{q}_2) = [F_1(Q^2)\gamma_5 + F^2(Q^2)(\not{q}_1 + \not{q}_2)\gamma_5] \qquad (13)$$

and choose the Q^2 dependence of F_1 and F_2 to agree with the form-factor results of Ref. 4 for large Q^2. Since these results are proportional to $1/Q^2$, we need to modify this behavior for small Q^2. We take F_1 and F_2 to be constant for $Q^2 \leq 0.5$ GeV^2. Thus,

$$F_1(Q^2) = N_\pi F_{\rm em}(Q^2) = N_\pi \frac{8\pi\alpha_s(Q^2) f_\pi^2}{Q^2}, \quad Q^2 \geq 0.5 \text{ GeV}^2$$
$$= F_1(0.5 \text{ GeV}^2), \quad Q^2 \leq 0.5 \text{ GeV}^2 \tag{14}$$
$$F_2(Q^2) = \frac{\rho}{m_q} F_1(Q^2) .$$

The choice for small Q^2 is obviously arbitrary, though reasonable, but we shall obtain predictions which are independent of the small-Q^2 behavior of F_1 and F_2 and will point out which predictions these are. Two parameters have been introduced in Eq. (14), N_π which fixes the strength of the coupling (of F_1) and ρ which fixes the strength of F_2 relative to F_1. We will determine the relevant combination of N_π and other coupling constants when we estimate the normalization.

Variations in ρ have little effect on the results we will present; it is set equal to one in the computation. As for what the appropriate Q^2 is in $F_{1,2}(Q^2)$, it should reflect how far off shell is the highly virtual q or $\bar{q}$. For L_1 and L_3 of Fig. 2, we use $Q^2 = (2q_1 \cdot p_2 - m_\pi^2)$, $(2q_2 \cdot p_2 - m_\pi^2)$, respectively, and for L_2 we take $Q^2 = \max\{|q_1 \cdot K|, |q_2 \cdot K|\}$.

Once we have the $\pi q\bar{q}$ vertex, the calculation proceeds as it did in the photoproduction case. We write the amplitude in the same way as in Eq. (5), but with C_π given by

$$C_\pi = -\tfrac{2}{9} g_\phi^2 g_s^4 . \tag{15}$$

The right-hand side of the diagrams is the same in the pion- and photon-induced processes and therefore $\mathcal{R}^{\nu\lambda}$ is again given by Eq. (7). The left-hand side of course is different, leading to different $L_{i\,--}$, to be calculated from Fig. 2 with the incident photon replaced by a pion with vertex given by Eq. (13). The L_i's are then

$$L_{1\,--} = (-2q_{2-})[-2q_1 \cdot p_2 + m_\pi^2 + i\varepsilon]^{-1}[2q_2 \cdot k_1 + k_1^2 + i\varepsilon]^{-1}$$
$$\times \bar{u}(q_1)[F_1(1) + F_2(1)(2\not{q}_1 - \not{p}_2)]\gamma_5(\not{q}_1 - \not{p}_2 + m_q)\gamma_{-} v(q_2) ,$$
$$L_{2\,--} = [2q_2 \cdot k_1 + k_1^2 + i\varepsilon]^{-1}[2q_1 \cdot k_2 + k_2^2 + i\varepsilon]^{-1}\bar{u}(q_1)\gamma_{-}(\not{q}_1 + \not{k}_2 + m_q)$$
$$\times [F_1(2) + F_2(2)(2\not{q}_1 + 2\not{k}_2 - \not{p}_2)]\gamma_5(-\not{q}_2 - \not{k}_1 + m_q)v(q_2), \tag{16}$$
$$L_{3\,--} = (2q_{1-})[2q_1 \cdot k_1 + k_1^2 + i\varepsilon]^{-1}[-2q_2 \cdot p_2 + m_\pi^2 + i\varepsilon]^{-1}$$
$$\times \bar{u}(q_1)\gamma_{-}(\not{p}_2 - \not{q}_2 + m_q)[F_1(3) + F_2(3)(\not{p}_2 - 2\not{q}_2)]\gamma_5 v(q_2) ,$$

where the arguments of F_1 and F_2 are those appropriate for the three different L_i, as discussed above. The amplitudes $\mathfrak{M}_i$ are then obtained in exactly the same way as in KDR, yielding

$$\mathfrak{M}_1 = -\frac{i}{4(2\pi)^4} C_\pi \left(\frac{s}{2}\right)^{1/2} [q_1 \cdot p_2 - m_\pi^2/2]^{-1} g_1 \bar{u}(q_1)[F_1(1) + F_2(1)(2\not{q}_1 - \not{p}_2)]\gamma_5(\not{q}_1 - \not{p}_2 + m_q)\gamma_{-} v(q_2) ,$$
$$\mathfrak{M}_3 = -\frac{i}{4(2\pi)^4} C_\pi \left(\frac{s}{2}\right)^{1/2} [q_2 \cdot p_2 - m_\pi^2/2]^{-1} g_1 \bar{u}(q_1)\gamma_{-}(\not{p}_2 - \not{q}_2 + m_q)[F_1(3) + F_2(3)(\not{p}_2 - 2\not{q}_2)]\gamma_5 v(q_2) , \tag{17}$$
$$\mathfrak{M}_2 = \frac{i}{4(2\pi)^4} C_\pi \bar{u}(q_1)[g_2\Gamma_1 + g_3^\mu \Gamma_{2\mu} + 2F_2(2)(q_{1-} - q_{2-})g_4\gamma_{-}\gamma_5]v(q_2) ,$$

where

$$\Gamma_1 = \gamma_{-}(\not{q}_1 + \not{K}/2 + m_q)[F_1(2) + F_2(2)(2\not{q}_1 + \not{K} - \not{p}_2)]\gamma_5(-\not{q}_2 - \not{K}/2 + m_q)\gamma_{-} ,$$
$$\Gamma_2^\mu = F_1(2)p_{2-}\gamma_{-}\gamma^\mu\gamma_5 + F_2(2)(2q_{2-}q_1^\mu + p_{2-}K^\mu)\gamma_{-}\gamma_5 , \tag{18}$$

and the g_i are the same as in Eq. (11). A little algebra leads to

$$\mathfrak{M} = \frac{i}{4(2\pi)^4} C_\pi [A\bar{u}(q_1)\gamma_5 v(q_2) + B\bar{u}(q_1)\not{K}\gamma_5 v(q_2) + C\bar{u}(q_1)\gamma\cdot\gamma_5 v(q_2) + D^\mu \bar{u}(q_1)\gamma\cdot\gamma_\mu\gamma_5 v(q_2)] ,$$

$$A = s\left\{g_1\left[\frac{x_2 F_1(1)}{q_1\cdot p_2 - m_\pi^2/2} - \frac{x_1 F_1(3)}{q_2\cdot p_2 - m_\pi^2/2}\right] - 2g_2 F_1(2) x_1 x_2\right\} ,$$

$$B = \left(\frac{s}{2}\right)^{1/2}\left\{g_1\left[\frac{F_1(1)}{q_1\cdot p_2 - m_\pi^2/2} + \frac{F_1(3)}{q_2\cdot p_2 - m_\pi^2/2}\right] + g_2 F_1(2)(x_2 - x_1)\right\} , \tag{19}$$

$$C = \left(\frac{s}{2}\right)^{1/2}\left\{-g_1\left[\frac{2q_2\cdot K + t}{q_1\cdot p_2 - m_\pi^2/2} F_2(1) + \frac{2q_1\cdot K + t}{q_1\cdot p_2 - m_\pi^2/2} F_2(3)\right]\right.$$
$$\left. + 2g_2 F_2(2)[x_1 q_2\cdot K - x_2 q_1\cdot K + (x_1 - x_2)t/4] + F_2(2) g_3^\mu (2x_2 q_{1\mu} + 2x_1 q_{2\mu} + K_\mu) + 2(x_1 - x_2) g_4 F_2(2)\right\} ,$$

$$D^\mu = \left(\frac{s}{2}\right)^{1/2} F_1(2) g_3^\mu .$$

Standard trace techniques and some additional algebra then yield

$$\sum_{\text{spins}} |\mathfrak{M}|^2 = \left(\frac{C_\pi}{4(2\pi)^4}\right)^2 \{2M^2 A^2 + 8AB(s/2)^{1/2}(x_2 q_1\cdot K - x_1 q_2\cdot K) + 8AC m_q (s/2)^{1/2} + 8(s/2)^{1/2} AD^\mu (x_1 q_{2\mu} - x_2 q_{1\mu})$$
$$+ 4s x_1 x_2[-B^2 t + 2BD^\mu K_\mu + C^2 - D^\mu D_\mu]\} , \tag{20}$$

with $A-D$ given in the preceding equation.

In the photoproduction calculation, KDR found that their results were insensitive to the exact form of the right-hand side, the proton-elastic two-gluon form factor, and in their numerical computations used a phenomenological form. We use the same procedure, letting

$$(2\pi)^{-2}[I_1(k') - I_2]$$
$$\to F(\vec{k} \equiv \vec{k}' - \vec{K}/2, t) = F_0 e^{bt} \frac{\vec{k}\cdot(\vec{k} + \vec{K})}{(a + \vec{k}^2)} . \tag{21}$$

This general form was chosen in order to preserve the qualitative behavior of $I_2(k') - I_1$, Eq. (8), with the exponential t dependence introduced in order to conform to the empirical diffractive t dependence. (Recall that $[I_1(k') - I_2]$ was obtained from an elementary target scalar or pseudoscalar.) In the computation we set $b = 2.5$ GeV^{-2}, $a = 0.6$ GeV^2, as in KDR.

All the constant factors and unknown coupling constants can then be factored out of the invariant amplitude

$$\sum |\mathfrak{M}|^2 \equiv \left(\frac{C_\pi}{4(2\pi)^4}\right)^2 [(2\pi)^2 F_0]^2 N_\pi^2 \sum |\overline{\mathfrak{M}}|^2 \tag{22}$$

and the differential cross section is given by

$$\frac{d\sigma}{dM^2 d\cos\theta^*} = \frac{1}{s(s - M^2)} \times \int d\phi^* dt \left(\frac{1}{2^2 3^4 (2\pi)^2} \alpha_s^4 \alpha_\phi^2 N_\pi^2 F_0^2\right) \times \sum |\overline{\mathfrak{M}}|^2 . \tag{23}$$

It is possible to obtain a crude estimate of the combination of coupling constants and normalizations appearing in Eq. (23) if one is willing to believe that the (forward) elastic-scattering amplitude is dominated by graphs which are two-gluon reducible in the t channel, which may not be entirely unreasonable.[8] Details of the estimation are given in the Appendix. The result obtained is

$$\frac{d\sigma}{dM^2 d\cos\theta^*} = (2.8\ \mu\text{b/GeV}^2) \frac{1}{s(s - M^2)} \times \int dt \sum |\overline{\mathfrak{M}}|^2 \tag{24}$$

for either a quark or an antiquark jet at angle θ^*. The normalization should not be taken very seriously; it is included as an indication of the feasibility of measuring this cross section.

The integrals in Eq. (24) were evaluated numerically, and the resulting cross sections for $s = 300$ GeV^2 and various M^2 are plotted as functions of $\cos\theta^*$ in Fig. 4. We include predictions integrated

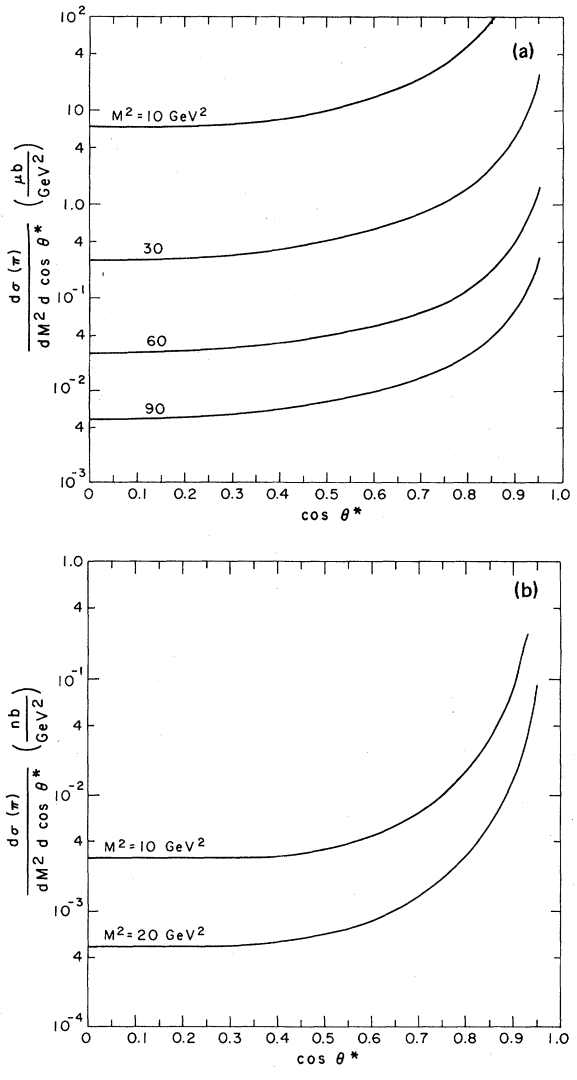

FIG. 4. Predictions for $\pi p \to q\bar{q}p$ at $s = 300$ GeV^2, including estimated normalization: (a) integrated over all t, (b) integrated over $t < 2$ GeV^2.

over large t ($|t| > 2\,\mathrm{GeV}^2$) because, as mentioned in the Introduction and explained in KDR, our use of perturbation theory is on firmer ground if $|t|$, as well as M^2, is large. Features of these results and comparison to the photoproduction predictions will be discussed in the next section.

IV. DISCUSSION

A. General features and comparisons

Not surprisingly, the general features of our predictions for pion-diffractive dissociation into $q\bar{q}$ are quite similar to the photoproduction results. For large s/M^2, the cross sections are approximately independent of s at fixed M^2. This can be seen from Eqs. (19), (20), and (23). In addition, our normalization estimates indicate that the cross sections are sufficiently large to be measured. As noted in the Appendix, there is no dependence on ϕ^* (except near $\cos\theta^* = 1$) and, consequently, away from $\theta^* = 0$ there should be no correlation between the $\vec{p}_2 \times \vec{q}_i$ plane and the $\vec{p}_1 \times \vec{p}_3$ plane in the $\vec{q}_1 + \vec{q}_2 = 0$ frame.

The $\cos\theta^*$ dependence of the cross section is more complicated than it was in the photon-induced process. The qualitative behavior looks similar—forward peak, flat at wide angles—but the details are rather different. The forward peak is caused by the quark propagators and the pion form factor. Both lead to factors of $(q_i \cdot p_2 - m_\pi^2/2)^{-1}$ in the amplitude [cf. Eqs. (14) and (19)] which for large M^2 becomes

$$(q_i \cdot p_2 - m_\pi^2/2)^{-1} \simeq (4/M^2)[1 - \cos\theta^* + O(m^2/M^2)]^{-1}. \tag{25}$$

The peak is not as sharp as would result from these factors alone, which would lead to $(1 - \cos\theta^*)^4$ in the cross section, due to other factors which dip near $\cos\theta^* = 1$, e.g., x_2. The result is a peak, but not so sharp as one might naively expect. That the peak comes almost automatically from the quark propagator, that it occurs near $\cos\theta^* = 1$ where one of the invariants is small thereby removing the justification of lowest-order perturbation theory, and that the region near $\cos\theta^* = 1$ is where we are sensitive to the arbitrary choice [Eq. (14)] of $F_\pi(Q^2)$ for small Q^2, all vitiate use of the near forward region as a significant test of the underlying dynamics. The predictions of Figs. 3 and 4 are only reliable for $\cos\theta^* \lesssim 0.9$.

While all the features (s, ϕ^*, M^2, and $\cos\theta^*$ dependence) mentioned above constitute tests of our assumptions (color-singlet exchange, QCD perturbation theory, pion form factor), the test which is most selective and reliable is the M^2 dependence, either at fixed $\cos\theta^*$ or integrated over the flat portion of the $\cos\theta^*$ spectrum. This is presented in Fig. 5 for a representative range of $\cos\theta^*$ and M^2 at $s = 300$ GeV^2.

An interesting comparison is the ratio of the pion-induced to the photon-induced cross section, attempting to exhibit manifestations of the pion's composite structure as opposed to the photon's elementary nature. One expects that the M^2 dependence at large angles should reflect the qualitatively different couplings of the two to $q\bar{q}$, and so in Fig. 6 we plot the ratio of pion- to photon-induced cross sections as a function of M^2 at fixed angle. As in Fig. 5, these predictions are sensitive only to the large Q^2 $\pi q\bar{q}$ or $\gamma q\bar{q}$ vertices. The M^2 dependence is weaker than the M^{-4} which one might expect from the pion form factor alone. This is due to cancellations which occur in the

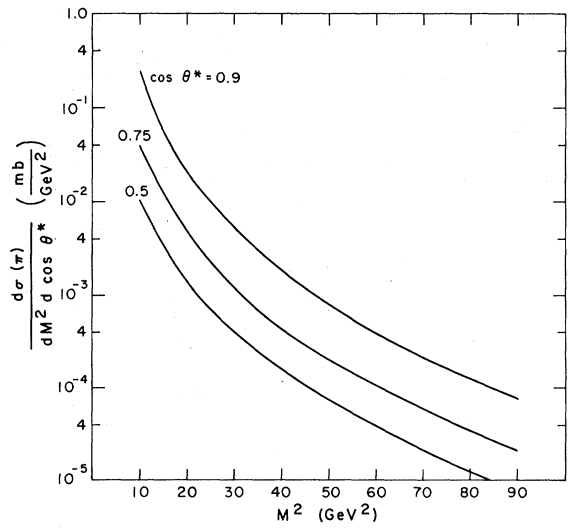

FIG. 5. Dependence on M^2 of the pion-diffractive-dissociation cross section at fixed $\cos\theta^*$ for $s = 300$ GeV^2 and integrated over all t.

photon, but not the pion, case. These cancellations result in the photoproduction cross section falling faster than the $1/M^2$ which would be expected from purely dimensional considerations (applied to $\Sigma|\mathfrak{M}|^2$).

The other obvious comparison one might try is to look for different angular dependences at fixed M^2. The pion cross secion should fall more rapidly away from $\cos\theta^* = 1$. Quantitative comparison, however, is not very reliable due to the problems mentioned above for the pion fragmentation and the analogous problems for photoproduction, including the presence of vector-dominance effects at small θ^*.

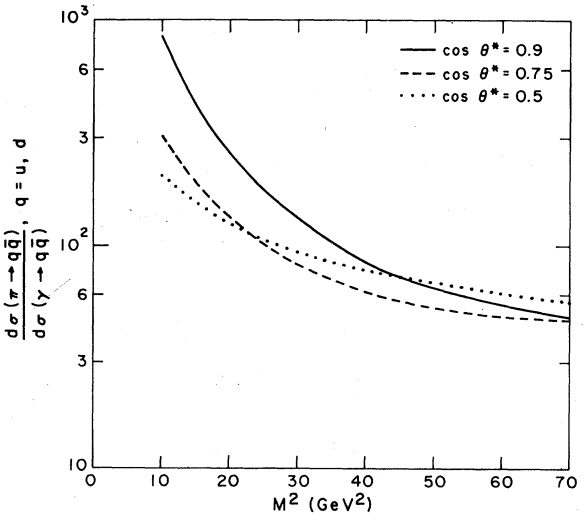

FIG. 6. Ratio of pion-induced to photon-induced cross sections integrated over all t, fixed $\cos\theta^*$ and $s = 300$ GeV^2.

B. Significance

In principle, measurement of this (and the photon-induced) process will provide a number of tests of QCD. The most basic feature being tested is the non-Abelian nature of the theory. The fact that a single gluon carries color, whereas protons do not, was what required at least two gluons to couple to the target plus recoil proton system. Exchange of one color-octet gluon would result in two octets (pion plus gluon and proton minus gluon) recoiling from one another, which through the soft long-range confining mechanism does not give rise to large gaps in momentum space. To be a little more precise then, the exchange of two gluons follows from the gluons carrying color plus the assumption that large gaps in rapidity can be treated perturbatively. The use of perturbation theory in treating large rapidity gaps has been considered in e^+e^- annihilation,[3] where it was found to be justified for $x \neq 0, 1$, which for the present calculation is $\cos\theta^* \neq 1$. Therefore, the fact that two-gluon exchange is the lowest-order contribution is required by and is peculiar to non-Abelian theories.

How then does one distinguish experimentally between one- and two-gluon exchange? The most obvious difference is in normalization: One-gluon exchange would be larger by a factor of about $1/\alpha_s(M^2)$ for small t. Our crude normalization estimate may be accurate enough to use this test, but a more direct comparison is the measured cross sections for events with versus those without the large gap. One- (Abelian) gluon exchange would lead to the two being equal (modulo phase space), whereas QCD suppresses the large gap events by an extra $\alpha_s(M^2)$. Other differences between one- and two-gluon exchange, and consequently between Abelian and non-Abelian gluons, occur in the $\cos\theta^*$ and M^2 dependence of the cross section. Although the graphs L_1 and L_3 of Fig. 2 can behave similarly to one-gluon exchange, the graph L_2 leads to differences, especially for larger θ^*.

This process also tests other features of QCD. Different gluon spin would lead to different s dependence and presumably to different $\cos\theta^*$ and M^2 dependence. In addition, the M^2 dependence (and to a lesser extent the $\cos\theta^*$ dependence) is sensitive to the QCD predictions for the pion form factor.[4] This is not a very good test, however, since it would be very difficult to determine the presence or absence of the logarithm in Eq. (14), which is all that distinguishes the Q^2 dependence

in QCD from the general power-counting result[9] common to other theories as well.

C. Summary

We have calculated the cross section for diffractive dissociation of the pion into a high-mass state in cases where the final-state fragments of the pion can be clearly separated from any other debris. The normalization estimates indicate that the cross section is measurable, so that the predictions can be tested in practice. When the fragments are analyzed in their collective rest frame, they should exhibit jet behavior, and the angular distribution for the jets was obtained. In addition, the s and M^2 dependences were calculated, the latter reflecting the pion form factor. The ratio of pion to photon fragmentation as a function of M^2 constitutes an instructive demonstration of the nonfundamental nature of the pion. Obviously, a similar analysis could be applied to kaon diffractive dissociation as well, and it would differ only in minor details from the present work.

ACKNOWLEDGMENTS

I am grateful to G. Farrar, G. Sterman, and U. Nauenberg for conversations helpful to this and to the previous related paper (Ref. 1), and to A. Donnachie and S. King for conversations and correspondence. This work was supported by the U. S. Department of Energy under Grant No. DE-AC02-76ER02114.

APPENDIX: NORMALIZATION

We first estimate the photoproduction normalization. Recalling that the phenomenological form for $[I_1(k')-I_2]$, Eq. (21), is used in all the numerical computations, we can extract a constant factor from the amplitudes squared by defining

$$\tfrac{1}{2}\sum|\mathfrak{M}_\gamma|^2 \equiv \frac{4}{27\pi}(2\pi)^4\alpha_{\rm em}\alpha_\phi{}^2\alpha_s{}^2Q_q{}^2F_0{}^2\tfrac{1}{2}\sum|\overline{\mathfrak{M}}_\gamma|^2\ , \tag{A1}$$

with Q_q the quark charge in units of e. The combination of coupling constants needed is thus $\alpha_s{}^4\alpha_\phi{}^2F_0{}^2$.

We can obtain a useful constraint if we assume that the proton elastic amplitude is given by Fig. 7, with the cross-hatched blob the same as in the text [cf. Fig. 1(b), Eqs. (7) and (21)]. The elastic scattering amplitude for our toy protons is then given by

$$\begin{aligned}\mathfrak{M}(\text{“}pp\text{”}) = &-\tfrac{1}{2}g_\phi{}^4\left(\frac{g}{2}\right)^4\left(\frac{1}{\sqrt{3}}\right)^4(\lambda_{ij}^{k'}\lambda_{ji}^{k}\lambda_{ab}^{k'}\lambda_{ba}^{k})\\ &\times\int\frac{d^4k'}{(2\pi)^4}[(k'+K/2)^2+i\epsilon]^{-1}\ [(k'-K/2)^2+i\epsilon]^{-1}\left\{\left(\frac{s}{2}\right)^{1/2}\delta(k_-')\frac{1}{2\pi}[I_1(k')-I_2]\right\}\\ &\times\left\{\left(\frac{s}{2}\right)^{1/2}\delta(k_+')\frac{1}{2\pi}[I_1(k')-I_2]\right\},\end{aligned} \tag{A2}$$

where the quantities in curly brackets are just $\mathfrak{R}^{--}\mathfrak{R}_{--}$ from Eq. (7) and the extra factor of $\frac{1}{2}$ is to (approximately) avoid double counting [cf. Fig. 1(b)]. If we replace $[I_1(k')-I_2]$ by the phenomenological form Eq. (21), the forward elastic amplitude becomes

$$\mathfrak{M}(\text{“}pp\text{”}, t=0) = -g_\phi{}^4g^4F_0{}^2\frac{s}{36a(2\pi)}\,. \tag{A3}$$

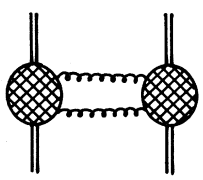

FIG. 7. General form assumed for pp elastic amplitude in order to estimate normalization.

With our conventions the optical theorem reads

$$\sigma_{\rm tot} = \frac{1}{|\vec{v}_1-\vec{v}_2|}\frac{1}{4E_1E_2}[-2\Re e\mathfrak{M}(t=0)]\ , \tag{A4}$$

so that, taking $\sigma_{\rm tot}(pp)\simeq 39$ mb,

$$\alpha_\phi{}^2\alpha_s{}^2(0)F_0{}^2 = 0.354a\ \text{mb}\ , \tag{A5}$$

where a is a parameter in the phenomenological proton vertex, taken to be 0.6 GeV^2, and the running coupling constant is evaluated at $t=0$.

Returning to the equation for the differential cross section,

$$\frac{d\sigma(\gamma \to q\bar{q})}{dM^2 d\cos\theta^*} = \frac{1}{2^6(2\pi)^4 s(s-M^2)} \times \int dt\, d\phi^* \left(\tfrac{1}{2}\sum |\mathfrak{M}_\gamma|^2\right), \quad \text{(A6)}$$

we note that since there is no ϕ^* dependence in $\sum|\mathfrak{M}|^2$, except near $\cos\theta^*=1$, the ϕ^* integral just gives a 2π. Furthermore, Eq. (A6) is for a quark at angle θ^*. The cross section for a jet (either q or $\bar{q}$) at θ^* is just twice this. Taking this into account, substituting Eq. (A5) into Eq. (A1), and using the numerical values $a=0.6$ GeV^2, $m_q=0.3$ GeV, one obtains

$$\frac{d\sigma(\gamma \to \text{jet})}{dM^2 d\cos\theta^*} = (16\ \text{nb/GeV}^2)\frac{1}{s(s-M^2)} \times \int dt\, \tfrac{1}{2}\sum |\mathfrak{M}_\gamma|^2 \quad \text{(A7)}$$

for the incoherent sum of $u+d$ quarks, where we have also taken α_s out of the integral, replacing it by an effective small-t value of one. (For large t we do use the running value in the integral.) This is the normalization used in the numerical predictions. Obviously, there is no compelling reason to really believe this, but it should be a reasonable indication of the approximate size of the cross sections we have calculated.

For the pion cross section, the combination of coupling constants which occurs is $\alpha_s^4\alpha_\phi^2 N_\pi^2 F_0^2$, cf. Eq. (23), which is just N_π^2 times the photoproduction combination estimated above. If we define $f_1 \equiv F_1(Q^2<0.5\ \text{GeV}^2)$ from Eq. (14), then the ratio of photon-proton total cross section to that of pion-proton should be given approximately by the ratio of their respective squared coupling constants to $q\bar{q}$, or

$$3\sum_q e_q^2 \Big/ f_1^2 \simeq \sigma_{\text{tot}}(\gamma p)/\sigma_{\text{tot}}(\pi p)\,, \quad f_1^2 \simeq 38.3\,. \quad \text{(A8)}$$

This fixes N_π^2, and repeating the remaining steps from the photoproduction estimate, we arrive at

$$\frac{d\sigma(\pi \to \text{jet})}{dM^2 d\cos\theta^*} = (2.8\ \mu\text{b/GeV}^2)\frac{1}{s(s-M^2)} \times \int dt \sum |\mathfrak{M}_\pi|^2\,, \quad \text{(A9)}$$

which is Eq. (24) of the main text.

[1] S. F. King, A. Donnachie, and J. Randa, Nucl. Phys. B167, 98 (1980).

[2] L. M. Jones and H. W. Wyld, Phys. Rev. D 17, 759 (1978); H. Fritzsch and K.-H. Streng, Phys. Lett. 72B, 385 (1978).

[3] J. Randa, Phys. Rev. D 21, 1795 (1980).

[4] G. R. Farrar and D. R. Jackson, Phys. Rev. Lett. 43, 246 (1979); S. J. Brodsky and G. P. Lepage, SLAC Report No. SLAC-PUB-2294, 1979 (unpublished).

[5] S.-J. Chang and S.-K. Ma, Phys. Rev. 180, 1506 (1969).

[6] Some of these results differ by about 10–25% from those of KDR near $\cos\theta^*=0$ due to an improvement in the numerical evaluation.

[7] E. Berger and S. J. Brodsky, Phys. Rev. Lett. 42, 94 (1979).

[8] F. E. Low, Phys. Rev. D 12, 163 (1975); S. Nussinov, Phys. Rev. Lett. 34, 1286 (1975); Phys. Rev. D 14, 246 (1976).

[9] S. J. Brodsky and G. Farrar, Phys. Rev. Lett. 31, 1153 (1973); Phys. Rev. D 11, 1309 (1975); V. A. Matveev, R. M. Muradyan, and A. N. Tavkhelidze, Lett. Nuovo Cimento 7, 719 (1973).